Structural Heterogeneity and Protein Composition of Exosome-Like Vesicles (Prostasomes) in Human Semen

Anton Poliakov,[1] Michael Spilman,[2] Terje Dokland,[2] Christopher L. Amling,[1] and James A. Mobley[1]*

[1]Department of Surgery/Urology, University of Alabama at Birmingham, Birmingham, Alabama
[2]Department of Microbiology, University of Alabama at Birmingham, Birmingham, Alabama

BACKGROUND. Human seminal fluid contains small exosome-like vesicles called prostasomes. Prostasomes have been reported previously to play an important role in the process of fertilization by boosting survivability and motility of spermatozoa, in addition to modulating acrosomal reactivity. Prostasomes have also been reported to present with sizes varying from 50 to 500 nm and to have multilayered lipid membranes; however, the fine morphology of prostasomes has never been studied in detail.
METHODS. Sucrose gradient-purified prostasomes were visualized by cryo-electron microscopy (EM). Protein composition was studied by trypsin in-gel digestion and liquid chromatography/mass spectrometry.
RESULTS. Here we report for the first time the detailed structure of seminal prostasomes by cryo-EM. There are at least three distinct dominant structural types of vesicles present. In parallel with the structural analysis, we have carried out a detailed proteomic analysis of prostasomes, which led to the identification of 440 proteins. This is nearly triple the number of proteins identified to date for these unique particles and a number of the proteins identified previously were cross-validated in our study.
CONCLUSION. From the data reported herein, we hypothesize that the structural heterogeneity of the exosome-like particles in human semen reflects their functional diversity. Our detailed proteomic analysis provided a list of candidate proteins for future structural and functional studies. *Prostate* © 2008 Wiley-Liss, Inc.

KEY WORDS: prostasomes; cryo-electron microscopy; proteomics

INTRODUCTION

Prostasomes are small lipid membrane-confined vesicles present in large quantities in human semen [1] and semen from male animals of several species [2,3]. Prostasomes have been shown to play an important role in the process of fertilization. They increase sperm motility [4–6] and delay acrosomal reaction so that it would not occur prior to reaching the egg [7]. Prostasomes have also been reported to be immunosuppressive, which is important in preventing sperm destruction by the female's immune system. These functions are most likely achieved by direct interaction of prostasomes with spermatozoa [8,9] and immune system components present in female reproductive organs. Several complement regulation molecules have also been reported to be present on prostasomes: CD59 (membrane attacking complex inhibitor [10]), CD46 (membrane cofactor protein, cofactor of Factor I-mediated proteolysis of C3b [11,12]) and CD55 (decay accelerating factor [12]). Additionally, complement factor C3 along with fibrinogen has been reported to

be phosphorylated by protein kinases present on prostasomes [13], resulting in altered activation of complement factor C3 [14]. Prostasomes are also known to inhibit mitogen-induced lymphoproliferation [15], phagocytosis and creation of free radicals by neutrophils and macrophages [16,17] and the migration of macrophages [18]. Finally, prostasomes are also known to contain components of coagulation system [19].

Previously, prostasomes and other exosome-like particles were studied by thin-section electron microscopy (EM) [10,15,20–23], scanning EM [12,24–27] and negative staining EM [28]. Prostasomes were shown to range in size from 50 to 500 nm and to have multilayered membranes [21,22]. Based on the electron density of the particles, prostasomes were described as either "light" or "dark" [22]. However, the fine morphology of prostasomes was never studied in detail, since the fixation, embedding and dehydration steps of traditional EM preparation methods are strongly detrimental to the integrity of membranous structures like prostasomes.

Unlike thin-section EM, cryo-EM preserves the sample in its native state, in the absence of dehydration and staining artifacts [29]. Furthermore, cryo-EM produces a projection through the entire three-dimensional (3D) sample volume with which the 3D structure of the specimen can be deduced.

We have studied the structure of sucrose gradient-purified seminal prostasomes by cryo-EM and were able to observe for the first time the fine details of prostasomes. We show that the prostasomes possess sub-vesicular internal and external structures in the form of daughter vesicles and depositions of dark substance that was not visible in glutaraldehyde fixed thin-section preparations. We found that prostasomes display significant morphological heterogeneity with several distinct structural types present.

In parallel with the structural analysis, we have performed proteomic analysis of the prostasomes and identified 440 proteins with high probability. Proteins known to be specific to both prostate and epididymis were detected, which, together with the structural data, suggested composite origin of exosome-like particles in human semen.

We postulate that the structural heterogeneity of prostasomes must translate into functional heterogeneity, with different types of prostasomes reflecting varied and specific functions. It is also possible that these structurally specific prostasomes originate from several male sexual organs (i.e., seminal vesicles, testicles, prostate). Our detailed proteomic analysis has provided a list of the milieu of proteins to be studied for a more detailed future structural and functional analysis of prostasomes, and the origin of these very interesting vesicles.

MATERIALS AND METHODS

Preparation of Prostasomes

Semen from three healthy volunteers was collected and left to liquefy at room temperature for 20 min. Cells and large pieces of undissolved seminal gel were removed by centrifugation at 1,000g for 10 min, and the supernatant was further centrifuged at 10,000g for 30 min to remove cellular debris and smaller pieces of undissolved seminal gel. The resulting supernatant was centrifuged at 100,000g for 2 hr, and the pelleted prostasomes were washed and redissolved in TBS buffer.

Prostasomes were further purified by sucrose gradient using step gradients of 0.3, 0.6, 0.9, and 1.3 M sucrose in TBS. The prostasome suspension was layered on the top of the sucrose gradient and centrifuged at 75,000g for 8 hr. An intense opaque prostasome band was collected by puncturing the tube from the side. The prostasome suspension was slowly diluted 6× with ice-cold TBS and pelleted at 100,000g for 30 min. The resulting pellet was used for all further experiments.

Electron Microscopy

For cryo-EM 3 μl of prostasomes was applied to C-flat holey film (Electron Microscopy Sciences), blotted briefly before plunging into liquid ethane and transferred to a Gatan cryo-sample holder. All samples were visualized in an FEI Tecnai F20 electron microscope operated at 200 kV, and images were captured on a 4 k × 4 k Gatan Ultrascan CCD camera at a magnification of 29,000×.

For obtaining tilt series, sample holder was tilted incrementally by 1° in both directions ± 60°. The images were taken at each angle at reduced beam intensity so that the total electron dose on the sample was below 100 e$^-$/Å^2.

For thin-section microscopy 2.5% glutaraldehyde in phosphate-buffered saline (pH 7.2). After fixation, the specimens were trimmed into a few smaller pieces and embedded in Epon to form plastic blocks according to conventional techniques. The plastic blocks were cut in 2 mm sections for light microscopy to find areas with neoplastic tissue. These areas were trimmed to be cut in 50 nm sections for ultrastructural examinations. The sections were put on slot grids with 0.5% Formvar film, contrasted with lead citrate and uranyl acetate, and examined in an electron microscope (FEI Tecnai F20).

Determination of Protein Composition of Prostasomes

A total of 100 μg of prostasomes (by protein) were loaded on a 12% SDS–PAGE gel and separated. The gel was stained with Coomassie and the gel lane was cut

into 15 strips. The proteins were reduced and alkylated with iodoacetamide. The strips were destained in 60% methanol, 0.1% trifluoroacetic acid (TFA) and dried with pure acetonitrile. The acetonitrile was removed by evaporation in a Speedvac centrifugal evaporator and protein digestion was performed by the addition of 10 µg/ml Trypsin Gold (Promega) solution in 100 mM ammonium bicarbonate and incubated for 8 hr at 37°C. After extraction with 10% acetonitrile, the peptides were loaded on a 100 nm × 10 cm capillary column in-house packed with C18 Monitor 100 A-spherical silica beads and eluted by a 1 hr gradient of 10–100% acetonitrile, 0.1% TFA. Mass spectrometric analysis was performed on an LTQ XL (Thermo Finnigan) spectrometer. The search for matching peptide sequences was performed using the SEQUEST search engine with UniProt database including mouse entries. The SEQUEST results were processed by Trans Proteomic Pipeline software and peptides with a probability of >0.6 were reported [30].

Classification of Protein Hits

UniProt protein IDs were enriched for GO terms using The Protein Information and Property Explorer (http://pipe.systemsbiology.net/pipe/#summary). Search and calculation of the number of proteins falling into different categories according to their cellular location and biological processes they take part in was performed using Excel spreadsheet.

RESULTS

Sucrose Gradient Purification of Prostasomes

Coarse prostasome preparations were purified from human semen by differential centrifugation. This preparation was shown to be contaminated by the previously termed "amorphous substance" [21,22], which is most likely residues of partially cleaved seminal gel (Poliakov A, unpublished results). In order to remove this contamination and to separate prostasomes from other undissolvable material, we separated the prostasomes further on sucrose gradients. A very intense, opaque band was observed at the 0.9/1.3 M sucrose interface and some precipitated material was also evident at the bottom of the tube. Material collected from the band was slowly diluted fourfold with isotonic TBS buffer and the particles were spun down at 70,000g for 1 hr. It was important to dilute the sample in high sucrose concentration slowly as it appeared that prostasomes are prone to disruption upon quick dilution, probably due to osmotic shock, as was witnessed by hard-to-resuspend pellet after harvesting prostasomes by ultracentrifugation. Microsocpic assessment of a thin section of glutaraldehyde-fixed

pellet revealed large, aggregated, elongated membranous structures (not shown) with few intact prostasomes. The washing procedure was repeated twice in order to remove any trace of sucrose that would produce strong background signal in cryo-EM.

Prostasomes Display Significant Morphological Diversity

The sucrose gradient-purified prostasomes were imaged by cryo-EM. In total, images of 301 vesicles were analyzed (Supplementary Figure 1A–F). Selected particles are presented in Figures 1–3. The particles generally varied in size from 50 to 200 nm, and only on occasion, were found to present as slightly larger. The overwhelming majority of particles were intact (Supplementary Figure 1D). All particles were confined by a trilamellar membrane. We classified the particles according to the four morphological criteria listed below:

(1) *Multiplicity of vesicles*: Most vesicles contained secondary, and occasionally, tertiary vesicles of smaller size (Fig. 1A), while a few vesicles appeared as singular entities (Fig. 2).
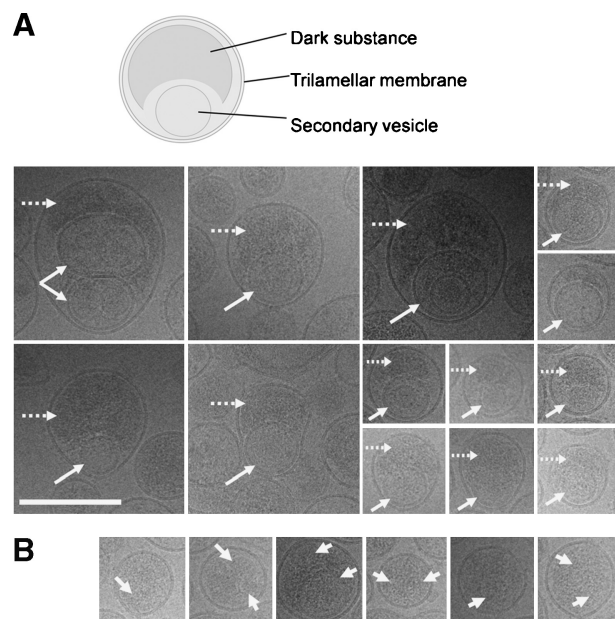(2) *Vesicle shape*: Most vesicles were close to round in shape, with some being completely round and

Fig. 1. Close-up view of high electron density vesicles. Cartoon representation is on top, showing general arrangement of structural elements in the vesicle. Dashed white arrows are showing dark depositions, solid white arrows are showing secondary vesicles. **A**: Projections of the vesicles where arrangement of secondary vesicles and dark depositions is clearly seen. **B**: Projections where secondary vesicles apparently overlay with dark depositions.
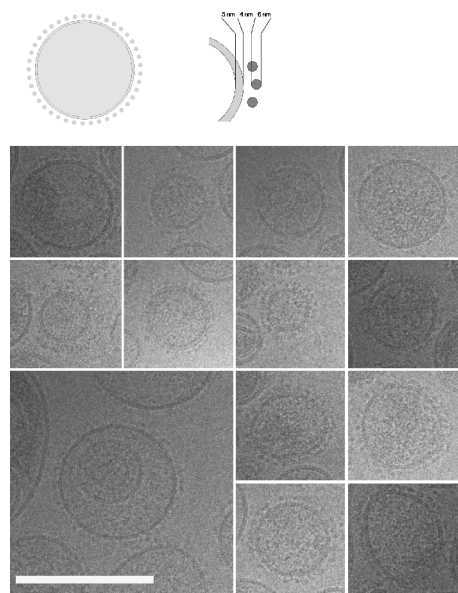
Fig. 2. Close-up view of low electron density particles with cauliflower-like protrusions. Cartoon to the left shows presence of surface depositions (protrusions) on the vesicle membrane. Cartoon to the right shows approximate distances between membrane and the blobs and the size of the later.

others egg-shaped (Figs. 1 and 2). However, few vesicles were distinctly elongated (Fig. 3), yet fully intact, meaning that they are not a result of vesicle rupture and emptying. Inspection of tilted images series showed that the elongated vesicles are sausage-shaped, rather than being side projections of erythrocyte-shaped particles (see below).
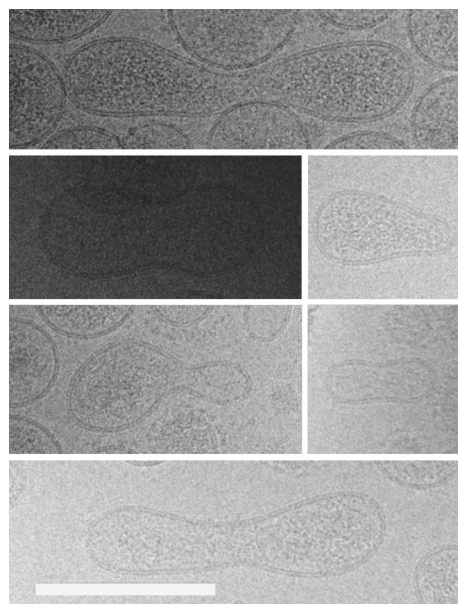

Fig. 3. Close-up view of selected elongated low electron density particles without cauliflower-like protrusions. White bar is 200 nm.

(3) *External Features*: Cauliflower-like protrusions measuring about 5 nm in diameter were clearly evident on some of the vesicles (Fig. 2), while other vesicles were devoid of them (Figs. 1 and 3). The globular protrusions were separated from the membrane by about 4 nm presumably via a stalk domain, and most likely correspond to membrane proteins. The density of the protrusions on the vesicle surface varied, with some vesicles being completely surrounded by the protrusions and some having large gaps in between them. However, the protrusions were rather uniform in appearance, suggesting that they correspond predominantly to a single type of protein. There was no apparent correlation between the presence of protrusions and the presence of secondary vesicles. However, larger vesicles tended to contain fewer protrusions and at lower density, and the largest vesicles were devoid of the protrusions all together.

(4) *Overall Density of Vesicles*: The electron density of the particles varied significantly. Inside some particles, a markedly electron dense substance was apparent (Fig. 1). This substance was usually generally organized into a sickle shape at one of the poles of the vesicle, being confined by daughter vesicles at another pole.

Using the above defined morphological criteria, we were able to distinguish at least three major types of particles as noted below

Type 1 (dark vesicles): High electron density vesicles with asymmetric deposition of dark substance surrounding one or more secondary vesicles (Fig. 1A). These particles are invariably smooth on the outside, lacking the cauliflower-like protrusions, and are nearly round or slightly elongated. Their sizes range from 100 to 200 nm. The fraction of these vesicles in the sample is around 50%. An exact count is complicated since the morphology of this type of particle is only obvious when it is seen in a projection depicted in Figure 1A. However, when viewed perpendicular to the horizontal axis of the view in Figure 1A, these particles will be much harder to recognize, as dark substance and the daughter vesicle will overlay. Particles depicted in Figure 1B are most likely of this type, with daughter vesicles barely visible due to the high density of the dark matter depositions.

Type 2 (light vesicles): Low electron density vesicles with abundant cauliflower-like protrusions (Fig. 2). These vesicles do not have internal depositions of dark substance, but sometimes contain daughter vesicles, and are nearly round or only slightly elongated. Their sizes range from 50 to 200 nm. This class represents approximately 25–30% of all vesicles.

Type 3: Low electron density vesicles without cauliflower-like features, presenting as elongated, or pear-shaped (Fig. 3), with no dark depositions, and smooth outer surface. They can be as long as 400 nm and about 50–100 nm wide. This class constitutes the remaining 20–25% of the vesicles.

In order to empirically determine if the above-described morphological features would be observable with thin-section EM we have further pelleted the purified fraction of prostasomes by ultracentrifugation and fixed the resulting pellet with glutaraldehyde. Thin sections were analyzed with transmission EM (Fig. 4). Both dark and light vesicles were observed in these sections, which has been described previously [22]. However, no protrusions on the outside surface of the vesicles were visible, and the arrangement of the dark substance in the vesicles was not obvious, though the particles indicated by the arrows in Figure 4 are likely the same dark vesicles that we have noted in our previous experiments. This offers the explanation for why the morphological features described in the present work were not described before with the use of thin-section EM.

We have noted that light vesicles remotely resemble mycoplasma (ureaplasma) cells [31]. According to the World Health Organization some 40–80% of all people are carriers of *Ureaplasma urealyticum* so it was important to establish that light vesicles are not ureaplasma cells. Proteomic analysis indicated that mycoplasmal protein is below detection (Supplementary Table II), which indicates that light vesicles cannot be ureaplasma or other mycoplasma cells.
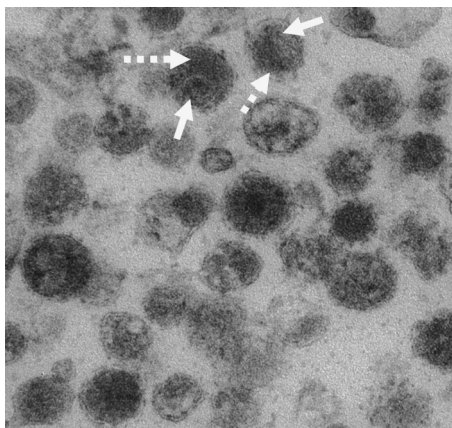

Fig. 4. Thin-section transmission EM image of prostasomes. White arrows indicate vesicles that look similar to the dark vesicles imaged in Figure IB. Dashed arrows indicate presumable dark depositions, solid arrows indicate secondary vesicle.

Confirmation of the Observed Structural Types of Prostasomes by Cryo-EM Tilt Series

In order to obtain information on the spatial arrangement of morphological elements and to further confirm the morphological types of prostasomes, we have collected a tilt series of images. To carry out these experiments, the sample holder with the frozen vesicles was incrementally tilted in 1–2° steps over an angular range of ±60° and images were taken at each angle. An animated view of the tilt series gives an idea of the 3D structure of the prostasome particles and is presented in Movies 1–3 that can be viewed at:

http://www.urology.uab.edu/urologyresearch/files/
    Movie1.avi

http://www.urology.uab.edu/urologyresearch/files/
    Movie2.avi

http://www.urology.uab.edu/urologyresearch/files/
    Movie3.avi

For better orientation in the animations dark and light prostasomes are indicated by dark and white arrows correspondingly on images taken at 0° from each animation (Supplementary MovieSnapshot1.tif— MovieSnapshot3.tif). The high electron density vesicles have clearly asymmetric deposition of the dark substance (Supplementary Movie 1 and Movie 3), which surrounds, rather than pushes, the daughter vesicles. It is clear from the tilt series that from some projections these particles look just like those in Figure 1B, and would not be distinguishable at these projections. The spacing between the dark substance and the membranes of the parent and daughter vesicles is constant and is about 4–5 nm.

Light vesicles were clearly visible and it was clear that the cauliflower-like protrusions completely cover the whole surface of the particles (Supplementary Mov.1–3). It was also obvious that there are no dark depositions in these particles as they were invariably transparent.

Elongated vesicles were clearly sausage-like and not side-projections of erythrocyte-like shapes (Movies 1–3). It was also clear that these vesicles are intact, ruling out a possibility of their shape being a result of rupture and partial emptying.

From animations of tilt series it is very clear that secondary and tertiary vesicles are indeed, inside of their parent particles and not simply overlay with them in the images (Supplementary Mov.1 and Mov.3). The daughter vesicles did not have any connection to the membrane of the parent vesicle and appeared to be "free-floating" and unconstrained inside them.

Protein Composition of Prostasomes

In order to study the protein composition of the prostasomes we have separated prostasomal proteins

by SDS–PAGE, cut the lane into 15 bands and performed trypsin in-gel digestion with each band. The resulting peptides were extracted and analyzed by nano-LC ESI MS/MS on an LTQ XL mass spectrometer (Thermo Finnigan). The resultant spectra were analyzed by three matching algorithms against a subset of the UniRef database specific for human proteins using SEQUEST (Thermo Finnigan), followed by the Pipeline software (ISB). Proteins identified with high confidence are listed in Supplementary Table. We have performed similar searches against a mycoplasma-specific database, and in stark contrast with the human database searches, no significant hits were present (Supplementary Table II), which strongly suggested that mycoplasmal contamination in the sample is minimal if present at all.

All matching algorithm output files were combined and analyzed with Pipeline software as mentioned, which reduces assignments of single spectrum to peptides from multiple proteins and calculates a probability for each peptide and protein. Using an empirically determined protein probability cutoff of 0.6 we obtained 440 protein hits, of which 304 were assigned with two or more peptides (Supplementary Table I). At this probability cutoff, only 15 proteins with probability <0.98 were predicted to be incorrectly assigned.

The data obtained here are not quantitative, that is, we cannot reliably tell the relative amounts of proteins present in prostasomes. However, the coverage and the number of successfully identified peptides (otherwise termed ''ion counting'') can give us rough measure of protein abundance. From Supplementary Table II it is clear that, for example, lactoferrin, aminopeptidase N, dipeptidyl peptidase IV, protein-glutamine gamma-glutamyltransferase 4, neprilysin, and various other proteins are highly abundant, which is witnessed by the high protein sequence coverage and high probability of the identified peptides.

Using The Protein Information and Property Explorer (http://pipe.systemsbiology net/pipe/#summary) (ISB), we have classified the identified proteins into groups according to several criteria, including cellular location (Supplementary Table I), molecular function and biological process they take part in. Of 440 proteins 73 proteins were non-annotated.

Most of the 440 identified proteins are assigned as intracellular. However, 32 proteins are known to be secreted. Most of these proteins are unlikely to be prostasome preparation contaminants, as all soluble proteins must have been efficiently excluded at ultracentrifugation and sucrose gradient steps. For example, prostate-specific antigen (present in normal human semen at concentration of approx. 1.2 mg/ml [32]) is not detected, which confirms that the purification protocol is efficient in removing soluble components of semen.

The presence of various secreted proteins including protease inhibitors is more easy to make sense of since they must be bound to their corresponding membrane proteases/peptidases identified in prostasomes, such as UniRef100_Q16651 (transmembrane protein), UniRef100_Q96KP4, UniRef100_P08473 (membrane metallo protease), UniRef100_P14384 (membrane protein), UniRef100_P15144 (membrane protein). Thus the protease inhibitors must be truly associated with prostasomes, albeit in an indirect way.

However, the presence of other proteins is not so easily explainable. Proteins that form seminal gel, semenogelin I and II and fibronectin, were detected with high confidence. These proteins constitute the bulk of the protein in ejaculate and are present at very high concentrations, so it is quite probable that they are a contamination, rather than a component of prostasomes. Soluble proteins should be very efficiently removed on sucrose gradient step; however, both semenogelins and fibronectin form a precipitate right after ejaculation, which slowly gets dissolved by prostate-specific antigen [33,34]. Our observations suggest that the dissolution is never fully complete, which means that semenogelin precipitates of different sizes must be present in the liquefied semen and some of them might co-purify with prostasomes.

DISCUSSION

Our work has provided the first glimpse at the fine structure of the exosome-like particles otherwise termed ''prostasomes'' and established cryo-EM as the method of choice for studying exosomes. Morphological diversity observed in prostasomes raises several important questions about the origin of prostasomes and their function.

The name prostasomes suggests that the vesicles are produced exclusively in the prostate and some claim this to be the case [1,24,35] but in other works the origin of prostasomes is suggested to be composite [36], which might be the case since semen is a product of five different organs: testes, epididymis, prostate, seminal vesicles, and Cowper gland. Indeed, exosome-like vesicles were observed in epididymis of men [18] and several other mammal species [37–43]. However, the relative abundance of the epididymal vesicles is likely low and, to our knowledge, their microscopic structure has never been studied. Additionally, no difference was observed in prostasomes size and number between semen from vasectomized and non-vasectomized individuals [44], suggesting that epididymosomes are present in insignificant quantities. So it is not possible to assign the structural types observed in this work to either prostate or epididymis. Proteomic analysis has revealed cystatin SA (UniRef100_P01034) and

dicarbonyl/L-xylulose reductase (UniRef100_Q7Z4W1) in the vesicle preparation: both proteins are abundantly expressed in epididymis, but not in prostate. This also suggests that some vesicles might indeed be of epididymal origin. But since proteomic data presented here are not quantitative it does not rule out relative scarcity of epididymosomes in semen.

In previous work [20] prostasome-like particles were observed in prostate tissue of men. They appeared very similar to the dark vesicles observed in the present work, with some vesicles clearly having secondary vesicles surrounded by dark substance (Figs. 2 and 8 in [20]), suggesting that at least dark vesicles have prostate origin. Other vesicles might still be a product of prostate too, reflecting excretion of mixed population of vesicles by prostate epithelial cells or functional heterogeneity of those cells. Study of pure prostate secretion is required to answer those questions.

Prostasomes were assumed to be produced in an exosome-like manner: first intracellular membrane budding into a multi-vesicular body and then fusion of the later with the cellular membrane and release of prostasomes. This mechanism can hardly explain how dark prostasomes are formed; specifically, how and why daughter vesicles are produced and how dark depositions occupy only just the space left outside of the daughter vesicles. It is plausible upon first inspection to assume that the dark depositions are of higher molecular density in addition to electron density, and therefore of higher rigidity than the daughter vesicles. In that respect it is rather odd that a presumably "softer" daughter vesicle pushes aside the presumed more rigid dark deposition as depicted in Figure 1, and this observation is clearly evident in tilt series animations. Rather, one may more feasibly conclude that the dark depositions are more fluid with a lower molecular density, potentially made up of more dilute high electron density material, thereby allowing them to easily form to any

shape, especially if these features are produced after the daughter vesicles are formed.

The discovery of sphingomyelin phosphodiesterase (UniRef100_Q5T0Y8) in the prostasomes might explain how secondary vesicles are formed. This enzyme has recently been implicated in the ESCRT-independent inward budding of exosomes into multivesicular exosomes originating from murine oligodendroglial cells [45]. Sphingomyelinase cleaves sphingomyelin into phosphocholine and ceramide, which has been shown to cause formation of secondary vesicles in giant unilamellar vesicles [45]. Prostasomes were shown to be rich in sphingomyelin [46,47] and sphingomyelinase activity might result in formation of secondary vesicles.

Equally enigmatic is how a second type of vesicle gets produced, that is, whether the noted features on the outside of the vesicles are acquired after the vesicles are formed or prior to budding into a multi-vesicular body. One plausible explanation is that this may occur following the liquefaction of semen with specific attachment of various protein(s) to the surface of light prostasomes. Of special interest is what these features are made of, as this would potentially provide a clue as to the function of the light prostasomes. The apparent size of these features (approx. 4–6 nm) suggests that this might be a single large protein molecule. For example, aminopeptidase N (UniRef100_P15144) fits well into this description, being a large membrane-bound protein [48] with dimensions of 85 Å × 56 Å (PDB entry 2DQM). Aminopeptidase N attaches to the lipid membrane at the N-terminus, with the main body of the protein presenting approximately 5 nm from the membrane [48], which fits well with what we have observed here (Fig. 2). Additionally, aminopeptidase N is clearly a very abundant protein in prostasomes (Supplementary Table I), being identified with 55 unique peptides covering 32.4% of its sequence. This
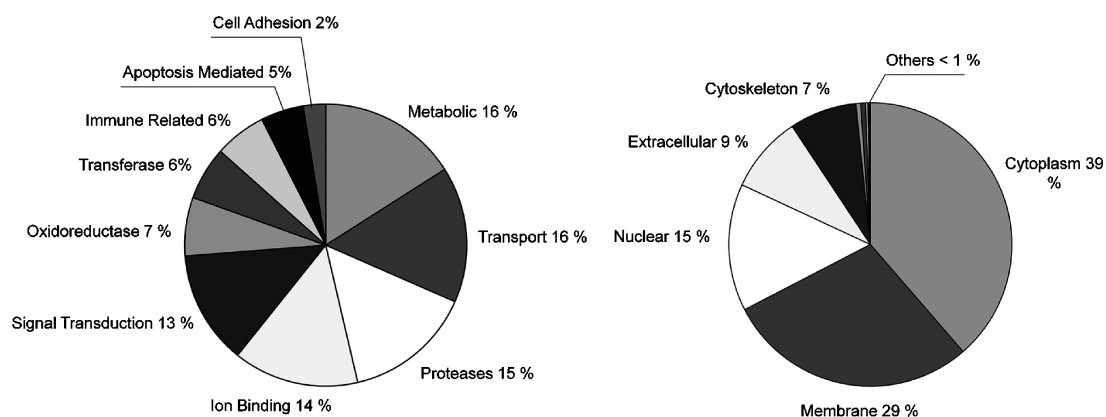

Fig. 5. Graphical representation of the protein groups present in prostasomes. **A**: Spatial distribution of the proteins. **B**: Distribution of the biological processes the proteins take part in.

protein was also previously described in prostasomes [8,49].

If the cauliflower-like features are indeed made up of aminopeptidase N (a cell-surface enzyme), then light vesicles might not be exosome-like, but rather being directly shed from the surface of the cell membrane (ectosomes).

Another important question is what the functions of the different structural types of prostasomes are as it seems quite probable that vesicles with such differing morphologies likely present with very different properties and functions, a point we hope to answer more definitively in future studies of this kind.

Proteomic analysis performed here has provided a large list of proteins that will be of great use for future studies on structure and function of prostasomes and, likely, for the discovery of new prostate cancer biomarkers. Discovery of two known candidate biomarkers of prostate cancer (prostate acid phosphatase (PAP) and prostate-specific membrane antigen (PSMA)) clearly demonstrates that prostasomes might be a valuable source of the biomarkers. Elucidation of spatial arrangement of PSMA and PAP (and other candidate biomarkers) in prostasomes and their association with one of the structural types of prostasomes would be of great practical value for usage of those biomarkers and understanding of their biology.

CONCLUSIONS

From the data reported herein, we hypothesize that the structural heterogeneity of the exosome-like particles in human semen reflects their functional diversity and, possibly, origin from several organs in addition to the prostate. Our detailed proteomic analysis provided a list of candidate proteins for future structural and functional studies.

REFERENCES

1. Ronquist G, Brody I, Gottfries A, Stegmayr B. An Mg2+ and Ca2+-stimulated adenosine triphosphatase in human prostatic fluid: Part I. Andrologia 1978;10(4):261–272.

2. Arienti G, Carlini E, De Cosmo AM, Di Profio P, Palmerini CA. Prostasome-like particles in stallion semen. Biol Reprod 1998; 59(2):309–313.

3. Piehl LL, Cisale H, Torres N, Capani F, Sterin-Speziale N, Hager A. Biochemical characterization and membrane fluidity of membranous vesicles isolated from boar seminal plasma. Anim Reprod Sci 2006;92(3–4):401–410.

4. Fabiani R, Johansson L, Lundkvist O, Ulmsten U, Ronquist G. Promotive effect by prostasomes on normal human spermatozoa exhibiting no forward motility due to buffer washings. Eur J Obstet Gynecol Reprod Biol 1994;57(3):181–188.

5. Fabiani R, Johansson L, Lundkvist O, Ronquist G. Enhanced recruitment of motile spermatozoa by prostasome inclusion in swim-up medium. Hum Reprod 1994;9(8):1485–1489.

6. Wang J, Lundqvist M, Carlsson L, Nilsson O, Lundkvist O, Ronquist G. Prostasome-like granules from the PC-3 prostate cancer cell line increase the motility of washed human spermatozoa and adhere to the sperm. Eur J Obstet Gynecol Reprod Biol 2001;96(1):88–97.

7. Cross NL, Mahasreshti P. Prostasome fraction of human seminal plasma prevents sperm from becoming acrosomally responsive to the agonist progesterone. Arch Androl 1997;39(1):39–44.

8. Arienti G, Carlini E, Verdacchi R, Cosmi EV, Palmerini CA. Prostasome to sperm transfer of CD13/aminopeptidase N (EC 3.4.11.2). Biochim Biophys Acta 1997;1336(3):533–538.

9. Arienti G, Polci A, Carlini E, Palmerini CA. Transfer of CD26/dipeptidyl peptidase IV (E.C. 3.5.4.4) from prostasomes to sperm. FEBS Lett 1997;410(2–3):343–346.

10. Rooney IA, Atkinson JP, Krul ES, Schonfeld G, Polakoski K, Saffitz JE, Morgan BP. Physiologic relevance of the membrane attack complex inhibitory protein CD59 in human seminal plasma: CD59 is present on extracellular organelles (prostasomes), binds cell membranes, and inhibits complement-mediated lysis. J Exp Med 1993;177(5):1409–1420.

11. Kitamura M, Namiki M, Matsumiya K, Tanaka K, Matsumoto M, Hara T, Kiyohara H, Okabe M, Okuyama A, Seya T. Membrane cofactor protein (CD46) in seminal plasma is a prostasome-bound form with complement regulatory activity and measles virus neutralizing activity. Immunology 1995;84(4):626–632.

12. Rooney IA, Heuser JE, Atkinson JP. GPI-anchored complement regulatory proteins in seminal plasma. An analysis of their physical condition and the mechanisms of their binding to exogenous cells. J Clin Invest 1996;97(7):1675–1686.

13. Babiker AA, Ronquist G, Nilsson B, Ekdahl KN. Overexpression of ecto-protein kinases in prostasomes of metastatic cell origin. Prostate 2006;66(7):675–686.

14. Ekdahl KN, Nilsson B. Alterations in C3 activation and binding caused by phosphorylation by a casein kinase released from activated human platelets. J Immunol 1999;162(12):7426–7433.

15. Kelly RW, Holland P, Skibinski G, Harrison C, McMillan L, Hargreave T, James K. Extracellular organelles (prostasomes) are immunosuppressive components of human semen. Clin Exp Immunol 1991;86(3):550–556.

16. Skibinski G, Kelly RW, Harkiss D, James K. Immunosuppression by human seminal plasma–extracellular organelles (prostasomes) modulate activity of phagocytic cells. Am J Reprod Immunol 1992;28(2):97–103.

17. Saez F, Motta C, Boucher D, Grizard G. Prostasomes inhibit the NADPH oxidase activity of human neutrophils. Mol Hum Reprod 2000;6(10):883–891.

18. Frenette G, Legare C, Saez F, Sullivan R. Macrophage migration inhibitory factor in the human epididymis and semen. Mol Hum Reprod 2005;11(8):575–582.

19. Lwaleed BA, Greenfield RS, Birch BR, Cooper AJ. Does human semen contain a functional haemostatic system? A possible role for tissue factor pathway inhibitor in fertility through semen liquefaction. Thromb Haemost 2005;93(5):847–852.

20. Brody I, Ronquist G, Gottfries A. Ultrastructural localization of the prostasome—an organelle in human seminal plasma. Ups J Med Sci 1983;88(2):63–80.

21. Stridsberg M, Fabiani R, Lukinius A, Ronquist G. Prostasomes are neuroendocrine-like vesicles in human semen. Prostate 1996;29(5):287–295.

22. Brody I, Ronquist G, Gottfries A, Stegmayr B. Abnormal deficiency of both Mg2+ and Ca2+-dependent adenosine

triphosphatase and secretory granules and vesicles in human seminal plasma. Scand J Urol Nephrol 1981;15(2):85–90.

23. Arienti G, Carlini E, Polci A, Cosmi EV, Palmerini CA. Fatty acid pattern of human prostasome lipid. Arch Biochem Biophys 1998; 358(2):391–395.

24. Nilsson BO, Jin M, Einarsson B, Persson BE, Ronquist G. Monoclonal antibodies against human prostasomes. Prostate 1998;35(3):178–184.

25. Bordi F, Cametti C, De Luca F, Carlini E, Palmerini CA, Arienti G. Hydrodynamic radii and lipid transfer in prostasome self-fusion. Arch Biochem Biophys 2001;396(1):10–15.

26. Vivacqua A, Siciliano L, Sabato M, Palma A, Carpino A. Prostasomes as zinc ligands in human seminal plasma. Int J Androl 2004;27(1):27–31.

27. Ronquist G, Nilsson BO, Hjerten S. Interaction between prostasomes and spermatozoa from human semen. Arch Androl 1990;24(2):147–157.

28. Llorente A, van Deurs B, Sandvig K. Cholesterol regulates prostasome release from secretory lysosomes in PC-3 human prostate cancer cells. Eur J Cell Biol 2007.

29. Dubochet J, Adrian M, Chang JJ, Homo JC, Lepault J, McDowall AW, Schultz P. Cryo-electron microscopy of vitrified specimens. Q Rev Biophys 1988;21(2):129–228.

30. Nesvizhskii AI, Keller A, Kolker E, Aebersold R. A statistical model for identifying proteins by tandem mass spectrometry. Anal Chem 2003;75(17):4646–4658.

31. Seybert A, Herrmann R, Frangakis AS. Structural analysis of Mycoplasma pneumoniae by cryo-electron tomography. J Struct Biol 2006;156(2):342–354.

32. Lynne CM, Aballa TC, Wang TJ, Rittenhouse HG, Ferrell SM, Brackett NL. Serum and semen prostate specific antigen concentrations are different in young spinal cord injured men compared to normal controls. J Urol 1999;162(1):89–91.

33. Robert M, Gagnon C. Semenogelin I: A coagulum forming, multifunctional seminal vesicle protein. Cell Mol Life Sci 1999; 55(6–7):944–960.

34. Lwaleed BA, Greenfield R, Stewart A, Birch B, Cooper AJ. Seminal clotting and fibrinolytic balance: A possible physiological role in the male reproductive system. Thromb Haemost 2004;92(4):752–766.

35. Ronquist G, Brody I, Gottfries A, Stegmayr B. An Mg2+ and Ca2+-stimulated adenosine triphosphatase in human prostatic fluid–part II. Andrologia 1978;10(6):427–433.

36. Renneberg H, Konrad L, Dammshauser I, Seitz J, Aumuller G. Immunohistochemistry of prostasomes from human semen. Prostate 1997;30(2):98–106.

37. Legare C, Berube B, Boue F, Lefievre L, Morales CR, El-Alfy M, Sullivan R. Hamster sperm antigen P26h is a phosphatidylinositol-anchored protein. Mol Reprod Dev 1999;52(2):225–233.

38. Frenette G, Sullivan R. Prostasome-like particles are involved in the transfer of P25b from the bovine epididymal fluid to the sperm surface. Mol Reprod Dev 2001;59(1):115–121.

39. Eickhoff R, Wilhelm B, Renneberg H, Wennemuth G, Bacher M, Linder D, Bucala R, Seitz J, Meinhardt A. Purification and characterization of macrophage migration inhibitory factor as a secretory protein from rat epididymis: Evidences for alternative release and transfer to spermatozoa. Mol Med 2001; 7(1):27–35.

40. Yanagimachi R, Kamiguchi Y, Mikamo K, Suzuki F, Yanagimachi H. Maturation of spermatozoa in the epididymis of the Chinese hamster. Am J Anat 1985;172(4):317–330.

41. Frenette G, Lessard C, Sullivan R. Selected proteins of ''prostasome-like particles'' from epididymal cauda fluid are transferred to epididymal caput spermatozoa in bull. Biol Reprod 2002;67(1):308–313.

42. Rejraji H, Sion B, Prensier G, Carreras M, Motta C, Frenoux JM, Vericel E, Grizard G, Vernet P, Drevet JR. Lipid remodeling of murine epididymosomes and spermatozoa during epididymal maturation. Biol Reprod 2006;74(6):1104–1113.

43. Fornes MW, Barbieri A, Cavicchia JC. Morphological and enzymatic study of membrane-bound vesicles from the lumen of the rat epididymis. Andrologia 1995;27(1):1–5.

44. Carlsson L, Ronquist G, Eliasson R, Egberg N, Larsson A. Flow cytometric technique for determination of prostasomal quantity, size and expression of CD10, CD13, CD26 and CD59 in human seminal plasma. Int J Androl 2006;29(2):331–338.

45. Trajkovic K, Hsu C, Chiantia S, Rajendran L, Wenzel D, Wieland F, Schwille P, Brugger B, Simons M. Ceramide triggers budding of exosome vesicles into multivesicular endosomes. Science 2008;319(5867):1244–1247.

46. Arvidson G, Ronquist G, Wikander G, Ojteg AC. Human prostasome membranes exhibit very high cholesterol/phospholipid ratios yielding high molecular ordering. Biochim Biophys Acta 1989;984(2):167–173.

47. Carlini E, Palmerini CA, Cosmi EV, Arienti G. Fusion of sperm with prostasomes: Effects on membrane fluidity. Arch Biochem Biophys 1997;343(1):6–12.

48. Bauvois B, Dauzonne D. Aminopeptidase-N/CD13 (EC 3.4.11.2) inhibitors: Chemistry, biological evaluations, and therapeutic prospects. Med Res Rev 2006;26(1):88–130.

49. Utleg AG, Yi EC, Xie T, Shannon P, White JT, Goodlett DR, Hood L, Lin B. Proteomic analysis of human prostasomes. Prostate 2003;56(2):150–161.